

This is an Open Access document downloaded from ORCA, Cardiff University's institutional repository: <https://orca.cardiff.ac.uk/id/eprint/113716/>

This is the author's version of a work that was submitted to / accepted for publication.

Citation for final published version:

Perni, Stefano, Yang, Lirong, Preedy, Emily Callard and Prokopovich, Polina 2018. Cobalt and Titanium nanoparticles influence on human osteoblast mitochondrial activity and biophysical properties of their cytoskeleton. *Journal of Colloid and Interface Science* 531 , pp. 410-420. 10.1016/j.jcis.2018.07.028

Publishers page: <http://dx.doi.org/10.1016/j.jcis.2018.07.028>

Please note:

Changes made as a result of publishing processes such as copy-editing, formatting and page numbers may not be reflected in this version. For the definitive version of this publication, please refer to the published source. You are advised to consult the publisher's version if you wish to cite this paper.

This version is being made available in accordance with publisher policies. See <http://orca.cf.ac.uk/policies.html> for usage policies. Copyright and moral rights for publications made available in ORCA are retained by the copyright holders.



Cobalt and Titanium Nanoparticles Influence on Human Osteoblast Mitochondrial Activity and Biophysical Properties of their Cytoskeleton

by

Stefano Perni ¹, Lirong Yang¹, Emily Callard Preedy ¹, Polina Prokopovich ^{1,*}

¹ School of Pharmacy and Pharmaceutical Sciences, Cardiff University, Cardiff, UK

word count abstract: 130

complete manuscript word count: 4821

number of references: 56

number of figures/tables: 9/1

* Corresponding author:

Dr. Polina Prokopovich e-mail: prokopovichp@cardiff.ac.uk

School of Pharmacy and Pharmaceutical Sciences

Cardiff University

Cardiff, UK, CF10 3NB

Tel: +44 (0)29 208 75820

Fax: +44 (0)29 208 74149

Abstract

We investigated the biophysical effects (cell elasticity and spring constant) caused on Saos-2 human osteoblast-like cells by nanosized metal (Co and Ti) wear debris, as well as the adhesive characteristics of cells after exposure to the metal nanoparticles. Cell viability was investigated using the MTT and LDH assays; along with metal uptake, cell apoptosis and mineralisation output (alizarin red assay) of the cells were also determined.

Osteoblasts viability was not affected by Ti nanoparticles at concentrations up to 1 mg/ml and by cobalt nanoparticles at concentrations < 500 mg/l; however elasticity and spring constant were significantly modified by the exposure to nanoparticles of these metals in agreement with the alteration of cell conformation (shape), as result of the exposure to simulated wear debris, demonstrated by fluorescence images after actin staining.

Keyword: Osteoblast, cobalt, titanium, nanoparticles, wear debris

Introduction

Osteoblasts and osteoclasts are cells involved in the synthesis (osteoblasts) and remodelling (osteoclast) of bone respectively [1]. The balance of these two actions is pivotal in osseointegration that is the process of bone deposition onto implanted biomedical devices such as those used in total joint arthroplasty [2].

Joint replacement devices are orthopaedic implants employed to return functionality to articulations that are damaged beyond their natural ability to self-repair. These devices present two abiotic surfaces that replicate the bone and cartilages of articulations. These surfaces originate debris in consequence of the wear that occurs during the movement of the joint. Depending on the chemical composition and size/shape, these wear debris can modify to the surrounding cells metabolism potentially leading to osteolysis and aseptic loosening of the device [3],[4].

Particles originated from the artificial joints have been retrieved the surrounding tissues of failed implants [5]-[8]. Debris are not only a factor contributing to periprosthetic osteolysis and aseptic loosening [8], but also increase the risk of infection [9]. Plenty of studies [5],[10]-[14] have investigated the biological impact of these wear particles on cells and tissues surrounding the implantation site [15]. There is also a general consensus over the higher danger posed by nanosized debris over microsized particles of the same material; likely linked to the greater ability of smaller particles to penetrate cell membrane [3].

In this study, Saos-2 cells were used as a model for human osteoblast. This cell line was derived from human osteosarcoma cells, and it is routinely employed as a model of human osteoblastic [1],[16],[17].

Many studies have investigated the effect of wear particle exposure on Saos-2 cells [18]-[22]; however there is a lack of understanding of the wear debris post-exposure impact on the nanoscale structural and biophysical properties of Saos-2 cells. The aim of this work was studying the elastic and adhesive properties of Saos-2 cells post exposure to Cobalt and Titanium nanoparticles. Additionally, mitochondrial activity (LDH and MTT) and apoptosis, calcium production activity of these cells, and the cell uptake were compared with biophysical data.

Results

Size and Charge of the nanoparticles

Both metal nanoparticles had negative zeta potentials (Table 1) with Titanium nanoparticles displaying the lowest overall negative charge at -44mV and with Cobalt nanoparticles having a potential of around -20mV. The human osteoblast also had a negative zeta potential of -7mV.

Mitochondrial activity

The mitochondrial activity (MTT data) of Saos-2 cells before and after exposure to Co and Ti nanoparticles for various time points is shown in **Figure 1**. After 24 hours all treated cells had a reduction in mitochondrial activity compared to the control cells, for 500 and 1000 $\mu\text{g/ml}$ Cobalt ($p < 0.05$). No difference was observed in the viability of cells exposed to Titanium nanoparticles even at the highest concentration of 1000 $\mu\text{g/ml}$ ($p > 0.05$).

After 48 hours, the overall viability values decreased for both untreated and treated cells. After exposure to Cobalt or Titanium nanoparticles the viability of Saos-2 cells (determined through MTT assay) did not differ from those of control sample ($p>0.05$) regardless of the concentration of the nanoparticles.

A similar trend was also recorded after the maximum exposure time of 72 hours when no difference in the measured cell viability was noticed for none of the tested concentrations of both Cobalt and Titanium nanoparticles ($p>0.05$).

LDH levels after 24 hours did not change greatly for Titanium particles, regardless the concentration ($p>0.05$). A slight reduction was however observed with Cobalt nanoparticles exposure for the highest concentrations of 500 and 1000 $\mu\text{g/ml}$ ($p<0.05$), with a reduction from 88% for the control cells to 72% at 500 $\mu\text{g/ml}$.

At 48 hours, Cobalt nanoparticle exposure had little to no alterations in LDH compared to the control ($p>0.05$), Saos-2 exposed to Titanium nanoparticles returned the same viability (LDH assay) as the control for all concentration tested ($p>0.05$).

After 72 hours of exposure, the control cells viability decreased to 56%. All exposed cells LDH levels had decreased viability too but no statistically significant differences were detected regardless of the type of nanoparticles or concentration ($p>0.05$).

Osteoblast mineralisation ability

To determine the mineralisation ability of the cells after exposure to nanoparticles the Alizarin red assay was used after 21 days of exposure to the nanoparticles. The control cells had an osteocalcin production value of 0.7 OD, shown in Figure 2. A general decrease in production was observed for both Cobalt and Titanium nanoparticles treated cells. For Cobalt nanoparticles the decrease was statistically significant in

comparison with the control samples at concentrations greater than 50 µg/ml. While for Titanium, only nanoparticles concentrations greater than 250 µg/ml gave results statistically different from the control samples ($p < 0.05$).

Biophysical properties

Elasticity and spring constant data are given in Figure 3 and Figure 4, respectively; each graph represents all time points that were measured at 24, 48, and 72 hours.

After 24 hours of metal nanoparticles exposure there was a general increase in elasticity i.e. the cells became stiffer with increasing concentrations of nanoparticles, and this was especially pronounced for Cobalt elemental nanoparticles. The initial elasticity for the control cells were at 9 kPa, for the lowest concentration the elasticity increased to 11 kPa for both Cobalt and Titanium nanoparticles, but this was not statistically significant ($p > 0.05$). However, a remarkable increase was observed at a concentration greater than 50 µg/ml for both Cobalt and Titanium nanoparticles ($p < 0.05$) After 24 hours exposed to the highest concentration of 1000 µg/ml of either titanium or cobalt nanoparticles the cells exhibited an elasticity almost double than of the unexposed cells.

With exposure time of 48 hours, the control cells remained consistent with an elastic modulus of 9 kPa, the same as the 24 hours. After exposure to Cobalt elemental nanoparticles the cells demonstrated no change in elasticity at a concentration of 5 µg/ml as observed at 9 kPa ($p > 0.05$); the elastic modulus of exposed cells increased thereafter for both titanium and cobalt.

The control cells had an elastic value of 13.5 kPa after 72 hour, greater than that recorded for the previous time points ($p > 0.05$). Again cells exposed to either cobalt or

titanium nanoparticles exhibited greater cell elasticity when the nanoparticles concentration was greater than 5 $\mu\text{g/ml}$.

Figure 4 represents the spring constant results for both Cobalt and Titanium nanoparticle exposure. At 24 hours, an obvious increase in spring constant was recorded with increasing concentration for both nanoparticles. The control spring constant was recorded at a value of 0.01 N/m; for Cobalt nanoparticles this value increased to 0.03 N/m at a concentration of 5 $\mu\text{g/ml}$, which remained the same for a concentration of 50 $\mu\text{g/ml}$. At the highest concentrations of 250, 500, and 1000 $\mu\text{g/ml}$ the spring constant values continued to increase to 0.05, 0.07, and 0.10 N/m, respectively. Titanium nanoparticle exposure also demonstrated a general increase in spring constant values but at smaller values than Cobalt nanoparticles; for 5 $\mu\text{g/ml}$ concentration the spring constant of the exposed cells was the same as the control value of 0.01 N/m, increasing to 0.03 N/m for concentrations of 50 and 250 $\mu\text{g/ml}$; at 500 $\mu\text{g/ml}$ gave a spike at 0.05 N/m which decreased to 0.04 N/m at 1000 $\mu\text{g/ml}$.

A similar pattern was observed for Cobalt nanoparticles exposed cells after 48 hours, but no change was recorded for Titanium nanoparticles. The control cells spring constant had increased to 0.02 N/m. For Cobalt nanoparticles the spring constant of the cells was not statistically different for concentrations of 50 and 250 $\mu\text{g/ml}$ ($p > 0.05$), and a dramatic increase was demonstrated at a concentration of 500 and 1000 $\mu\text{g/ml}$ at values of 0.11 and 0.13 N/m ($p < 0.01$). For the Titanium nanoparticles treated cells the values for the spring constant with was not different than the control samples ($p > 0.05$).

After 72 hours exposure to nanoparticles, there not an statistically significant difference between the control and exposed cells ($p > 0.05$).

Cell adhesion forces

For all cells, control cells (unexposed to nanoparticles), and exposed cells to Cobalt and Titanium nanoparticles adhesion data are given in Figure 5; the data demonstrated a non-Gaussian spatial distributions of adhesion forces on the cell surfaces.

At 24 hours, the median adhesive force recorded for the control cells was at 2.5 nN, the values for the Cobalt and Titanium nanoparticles exposed cells did not vary greatly from the control ($p>0.05$). After 48 hours, the control cells adhesion decreased to 1 nN compared to 24 hours control; for cells exposed to Cobalt nanoparticles the range of values of adhesion increased with increasing concentration, with the highest adhesion recorded at a concentration of 500 $\mu\text{g/ml}$ at 2.5 nN. For cells exposed to Titanium nanoparticles, the range of data was less than for cells exposure Cobalt nanoparticles ($p<0.01$) and the greatest adhesion was observed at 2.0 nN at a concentration of 5 $\mu\text{g/ml}$.

Three days of exposure demonstrated little to no change in adhesion force distribution for neither Cobalt nor Titanium exposed nanoparticles ($p>0.05$).

Metal uptake by cells

Metal uptake by cells data is shown in Figure 6. Regardless of the metal used, the uptake generally increased with increasing concentration after all three exposure times ($p<0.01$). For Cobalt nanoparticles, the maximum uptake was observed after 48 hours for 500 and 1000 $\mu\text{g/ml}$ concentrations at around 570 and 700 $\mu\text{g}/10^6\text{cell}$. For Titanium nanoparticles, the overall uptake was around six folds smaller than Cobalt nanoparticles, again after 48 hours exposure to the metal particles, demonstrated a peak of uptake especially for a concentration of 500 $\mu\text{g/ml}$ at around 90 $\mu\text{g}/10^6\text{cell}$.

After Ti nanoparticles exposure the cells demonstrated the greatest uptake at 24 hours with the greatest concentration after exposure to 1000 µg/ml Ti nanoparticles with an uptake of 110 µg/10⁶cell. No statistical difference between data after 48 and 72 hours for both types of particles (p>0.05).

Cell morphology

Osteoblast cell not exposed to any metal nanoparticles exhibited tubular filaments of actin in the cytoskeleton after 1 and 3 days of incubation. On the other hand the presence of Co induced conformational changes after 1 day of expose at nanoparticles concentration greater than 0.5 mg/ml with the cytoskeleton appearing more rounded; after 3 day of exposure to Co nanoparticles Saos-2 cells appeared similar to those in the control sample (no nanoparticles) at concentration below 1 mg/ml (Figure 7). Ti nanoparticles had a similar impact on the conformation of the actin in the cytoskeleton of Saos-2 cells (Figure 8).

Apoptosis

Saos-2 cells not exposed to any nanoparticles (control samples) exhibited a population of apoptotic cells of about 7-8 % (Figure 9) as determined by ANNEX. Once in contact with either cobalt or titanium wear debris simulating nanoparticles, the fraction of apoptotic cells increased with nanoparticles concentration and with exposure time. Furthermore, cobalt appeared to induce more apoptosis than titanium.

Discussion

Cobalt and Titanium nanoparticles used in this study resemble those retrieved from explants in terms of size and shape [12],[29]-[31]; this is critical in enabling the use of

these metal nanoparticles as model for joint replacement devices wear debris as particles morphology (i.e. size and shape) impacts proliferation and differentiation of cells along with wear particles concentration [29]. Particles with diameter smaller than 1 μm are more easily phagocytosed compared to larger counterparts [32] and elongated particles induce stronger cellular reactions than round particles [29],[33],[34]. Moreover, particles concentrations used in this study were the same range as studies and found in patient tissues [29],[35]. Moreover, no difference between Ti oxides and Ti elemental nanoparticles was found on the mitochondrial activity and mechanical properties of cells; [36],[37] similarly, Co oxide had the same effects as elemental Co [38]. Therefore the experimental conditions closely resemble in vivo situations.

Higher concentrations of Titanium (up to 10 mg/ml) were used with no noticeable cytotoxic effect by Pioletti *et al.* (1999) [15]; however they were shown to induce apoptosis [39]. Yet, similar concentrations of chromium and Cobalt-chromium induced cytotoxic effects with reduced bone formation [35]. This was also found in this investigation; for cells exposed to both Cobalt and Titanium, the bone mineralisation decreased with increasing concentration of nanoparticles after 21 days of growth (Figure 2).

It has been reported that the majority of titanium particles are phagocytosed in the first 24 hours [15]. This is in agreement with our results on the biophysical properties of cells that exhibited the greatest variation from the control sample after 24 hours of exposure (Figure 3, Figure 4, Figure 7, Figure 8). This was also observed for Cobalt nanoparticles in the investigation of human osteoblasts (Figure 6), however, there was no great change in the viability of the cells exposed to Titanium and these findings are

in agreement with the results presented by Vandrovcova *et al.* (2014) [40]. Moreover the apoptosis induced by both titanium and cobalt is well in agreement with previous studies [39] .

Osteoblasts surface properties also govern the osseointegration of an implant that is an essential process to ensure longevity and stability of implanted biomedical devices [3]. All metal particles used in this work had a negative zeta potential (Table 1), and it has been demonstrated that negatively charged surfaces increased the attachment to Saos-2 cells [40]. Despite the same electrostatic charge (both cells and nanoparticles were negatively charged), nanoparticles attached to the cells. This apparent violation of the electrostatic repulsion is often seen in biological samples and explained by the presence of adhering features on the cell external wall (proteins and other protruding filaments) that enable living cells to attach onto surfaces exhibiting the same charge as the cells despite the electrostatic repulsion [41] Cellular behaviour regulates the attachment of cells especially when concerned with osteoblast and fibroblasts as these cells need adherence for survival and growth [9],[42]. Others have suggested that the nanotopography of cells have an influence on cell behaviour governing the integrin clustering and focal adhesion assembly [43],[44].

The mechanical properties of single cells have been measured using various techniques [45]-[48], some of which include rheometry with magnetic beads, optical traps, and AFM [45]. Anchorage dependent cells can adapt to local physical stimuli by changing cell stiffness [43]; evidence of this has previously been observed using mesenchymal stem cells causing differentiation into specific lineage, for example, softer matrix induces neurogenic routes whereas stiffer matrices cause developments of myogenic and osteogenic phenotypes [43],[49],[50]. Alterations to the ECM can

influence further mechanical stimuli which impact on the cellular function, for example the growth, motility, survival, adhesion and contractility [51].

It has been noted that the elastic properties of osteoblasts are directly linked to the cytoskeleton [52],[53]; hence our results corroborate this as the changes in cytoskeleton structure observed through actin staining (Figure 7, Figure 8) are linked to the measured changes in the cell elasticity (Figure 3) and spring constant (Figure 4) and potential the initial stages of apoptosis as determined by annexin V assay (Figure 9) that is based on the exposure of a phospholipid-like phosphatidylserine (PS) on the outer cell membrane

Other studies have also used AFM techniques to investigate the stiffness of cells and reported that a cantilever spring constant of 0.06 N/m was sufficient to approach cellular samples of mammalian origin [54], correlating to the spring constant used for human osteoblasts in this study. Generally, it is accepted that differentiating cells are stiffer [45], for example Saos-2 cells not exposed to nanoparticles had a mean modulus of around 10 kPa while cells exposed to Cobalt exhibited an elastic modulus twice that of the control samples illustrating that metal nanoparticles do alter the cells mechanical properties. The elastic modulus of cells is of importance as, clinically, it has been suggested that changes to cellular stiffness indicate pathological disorders, for instance increased liver stiffness indicates cirrhosis [51]. Stiffness is therefore an important characteristic to explore as it indicates damage to the cells as represented by changes to the cytoskeletal organisation [51],[55]. It is believed that cytoskeleton is the main component of sensing mechanical changes [51],[55],[56]. Even though wear particles may not impact cell viability directly, they induce other mitochondrial and structural changes in the cells they affect as the cascade of event subsequent to

exposure to metal wear debris can be potentially deleterious to the long life of implanted joint replacement devices as shown here [36],[37].

Little to no change was observed in the MTT viability results for Saos-2 cells for both Cobalt and Titanium nanoparticle exposure (Figure 1), even though the same sized particles of Cobalt had a greater impact on the viability of the mouse MC3T3-E1 and cells [44],[37]. Interestingly, both Cobalt and Titanium nanoparticles increased the osteocalcin production in the mouse osteoblast cells but clear decreases in osteocalcin productions were observed for Saos-2 cells (Figure 2); the decrease in production suggests that damage to the cells viability of human osteoblast like cells must be present and was supported by the LDH viability assay (Figure 1). Additionally, cobalt induced more cell apoptosis than titanium (Figure 9) possibly linked to the lower uptake of the latter (Figure 6) and one of the reasons for the well-known cytocompatibility of titanium implants.

Similarly, the elasticity of cells exposed to either Cobalt or Titanium increased (Figure 3), demonstrating that cells become stiffer post exposure to metal wear debris validating the results concluded using mouse MC3T3-E1 osteoblast cells [37]; yet Cobalt in both cellular cases, MC3T3-E1 and Saos-2 induced greater increase in spring constants of the cells than Titanium (Figure 4). Also, the data regarding the adhesive forces increase with increasing concentration of nanoparticles observed in this study for human osteoblast expand such observation in other species (mouse osteoblast cells) [37]. The presence, therefore, of wear debris affects the normal function of the cells by the potential alterations to the essential cytoskeletal organisation which governs both the biophysical sensing and adhesive properties of living cells; this effect is generally without impact on cell viability. However, higher

levels of apoptotic cells were observed after exposure to simulated wear particles leading to the possibility that the impact of wear debris is more observable in a longer time window. Furthermore, the impact of the same conditions on murine osteoblast properties appeared to be more remarked than in human osteoblast [37].

Conclusions

Joint replacement devices are increasingly implanted in patients as their performance improves and the demand for such procedures is fuelled by aging population and growing incidence of risk factors (i.e. obesity). However, wear debris originated by the daily operation of these devices is the leading cause for their failure.

This work assessed the impact of simulated wear debris of joint replacement devices on both biophysical properties and cell behaviour of human osteoblast.

Our results demonstrated that cobalt nanoparticles accumulate into osteoblasts more than titanium and that such process induces immediate changes in the cell wall properties (elasticity and spring constant along with adhesive forces) without noticeable effects on the mitochondrial activity of the cells. However, both metal nanoparticles increase the population of cells exhibiting the initial stages of apoptosis (cobalt more than titanium) and thus suggesting that experiments carried out on short periods (few days) using viability assays such as MTT and LDH may not be the most appropriate to study the impact of wear debris.

As the performance of the currently commercially available joint replacement devices, mainly in terms of longevity that is still about 10-15 years and consequently still not satisfactory, new materials and technologies are under development to meet patients'

needs. Such development will be aided by the determination of wider and more appropriate testing conditions for the assessment of the impact of such new materials on osteoblast cells that this work provides.

Experimental

Nanoparticles

Elemental Co and Ti nanoparticles with average size of 30nm (Sigma Aldrich, UK). All nanoparticles were weighed and suspended in RPMI-1640 medium to make a stock solution of 5mg/ml.

Cell Culture

Saos-2 human osteosarcoma osteoblast-like cells (ATCC® HTB-85) were cultured in RPMI-1640 media, supplemented with 10% (v/v) Foetal Bovine Serum (FBS), 1% (v/v) of solution penicillin (5000 U/mL) and streptomycin (5000 mg/mL) (Gibco Invitrogen). Cells were incubated at 37°C, with 5% CO₂ humidified atmosphere.

For biophysical and adhesive properties measurements by the atomic force microscope (AFM), 60,000 cells were seeded in each well of 24-well plates containing a sterilised polystyrene slide. After incubation for 24 hours, Co or Ti nanoparticle were added from stock suspension to the final concentration of 5, 50, 250, 500, and 1000 µg/ml; then the plates incubated for the chosen time. The protocol was the same for cell uptake, osteoblast mineralisation ability, LDH and MTT assay and microscope imaging.

Mitochondrial activity assay

Saos-2 viability was assessed through MTT and Lactate dehydrogenase (LDH) assay (Sigma, UK). Cells were exposed to the metal nanoparticles as described before; after the desired exposure time, the media containing the metal nanoparticles was removed and the cells rinsed with sterile PBS. Media was replaced with 100 μ l of phenol red-free RPMI-1640 and 10 μ l of 5 mg/ml solution added; plates were then incubated for 4 further hours at 37°C in a humidified atmosphere containing 5% CO₂. 200 μ l of dimethyl sulfoxide (DMSO) were added in each well; after complete dissolution of the formazan produced, 200 μ l were transferred to a 96-well plate; absorbance at 560nm was measured using a spectrophotometer (ELISA Reader Labtech LT-500MS). Untreated cells (not exposed to any metal nanoparticles) were used as the control; all measurements were performed in triplicates.

For the determination of Saos-2 cells viability through LDH assay according to manufacturer's guidelines; 25 μ l of medium from each well where osteoblast were grown with/without nanoparticles were transferred into a 96-well plate containing 50 μ l of the freshly prepared LDH kit solution. The well plate stored in the dark for 30 minutes and absorbance at 490nm determined (ELISA Reader Labtech LT-500MS). For the total LDH levels, 100 μ l of LDH assay lysis was added to each well containing Saos-2 cells, after incubation for 45 minutes at 37 °C; 25 μ l from the well were transferred into a 96-well plate containing 50 μ l of the freshly prepared LDH kit solution. The well plate stored in the dark for 30 minutes and absorbance at 490nm determined (ELISA Reader Labtech LT-500MS).

Osteoblast mineralisation activity

Saos-2 cells were grown and exposed to the Co or Ti nanoparticles changing both the medium and nanoparticles twice a week. After 21 days, the medium was removed from all wells, cells were fixed with 10% (v/v) gluteraldehyde (Sigma Aldrich, UK) in sterile Phosphate Buffer Solution (PBS) (100 μ l) for 10 minutes at 37 °C. Then the gluteraldehyde solution was removed and cells were washed three times with PBS. Calcium was stained with 100 μ l of Alizarin red staining (ARS) (Sigma Aldrich, UK) (1 % w/v in distilled water) at 37 °C. After 20 minutes, ARS was removed and the wells washed with Milli-Q water; the staining was dissolved with 100 μ l of 10% Acetic acid (Sigma Aldrich, UK). After 30 minutes, 50 μ l from each wells were transferred into a 96-well plate and absorbance measurements carried out using a spectrophotometer (ELISA Reader Labtech LT-500MS) at a wavelength of 405nm [24]. All mineralisation tests were performed in triplicates.

Cell biophysical properties measurements

Atomic Force Microscopy (AFM) (XE-100 Advanced Scanning Probe Microscope (Park Systems, Korea) was used to determine the mechanical properties of cells; experiments were performed using an open liquid cell containing PBS as previously described [25]. Triangular tipless cantilevers (Bruker, UK) of nominal spring constants ($K_{cantilever}$) equal to 0.1 N/m were used; the actual spring constant of each individual cantilever was determined using the Sader method [26],[27]. Borosilicate glass beads (10 μ m in diameter) were glued onto the cantilever and served as cell indenter [36],[37]. Indentation depths >400-500 nm were avoided setting the maximum applied load to 4 nN, with the working load set at 2 nN. For each sample, at least 15 cells were analysed at each concentration of nanoparticles at each time point. Cells were first

located before at least 20 approaching and retracting z-piezo coordinates vs. deflection curves were obtained from casually selected points on the surface of each cell, attention was paid in avoiding the peri-nuclear area [36],[37]; all experiments were performed in triplicates.

Cell elasticity and spring constant determination

Cell biophysical properties were calculated through model fitting of the approaching part (trace) of the AFM curves [36],[37]. The Young modulus of the cell membrane location under investigation was estimated fitting the Hertz model (Eq. 1) to the part of the indentation vs. force curve after contact between AFM tip and cell surface [36],[37].

$$F = \frac{4}{3} \frac{E}{(1-\nu^2)} \sqrt{R} \delta^{2/3} \quad (1)$$

Where:

F = force recorded by AFM

E = Young modulus

R = radius of the spherical indenter (5 μm)

ν = Poisson ratio (set at 0.5)

δ = indentation depth

The spring constant exhibited by the cell surface in the location probed was, instead, calculated as the slope of the indentation curve after the Hertzian regime [36],[37], according to:

$$F = k_b \delta \quad (2)$$

Where:

$F =$ force recorded by AFM

$K_b =$ spring constant of the cell

$\delta =$ indentation depth

The separation between cell surface and AFM tip (δ), necessary for both models fitting, was estimated from the coordinates (z-piezo) of the trace curve offsetting the coordinated of the point of contact that was assumed to coincide with the local minimum of force [36],[37]:

$$\delta = |z - z_0| - d_{cant} \quad (3)$$

Where:

$z_0 =$ z-piezo value of the minimum of the trace curve

$z =$ z-piezo value of the trace curve

$d_{cant} =$ cantilever deflection

$\delta =$ indentation depth

and

$$F = K_{\text{Cantilever}} d_{\text{cant}} \quad (4)$$

All fitting calculations were carried out using an in-house written FORTRAN code employing the least squares method.

The heterogeneity of the biophysical cell surface properties was investigated through the spatial distribution of E and K_b .

Cell Adhesion force

The forces of adhesion between cells and AFM tip were determined as the minimum value of the retracting (retrace) part of the AFM curve.

Cell uptake of metal nanoparticles quantification

Cells were grown and exposed to the relevant nanoparticles for the required time period. Media was then removed from each well and the cells washed three times with PBS; 500 μl of Nitric acid were added and the plates were incubated at 60°C for further 24 hours. From each well 400 μl were removed and mixed with 8 ml of Milli-Q water in a polypropylene tube. The concentration of Ti or Co in this solution was measured using inductively coupled plasma-mass spectroscopy (ICP-MS) Optima 2100DV OES (Perkin Elmer, Waltham, MA, USA) calibrated with standard element Primar 28. The sample rate for the ICP-MS was 1.5 ml/min with characteristic wavelengths for each metal used: 288.616 nm for cobalt and 334.940 nm for titanium. Experiments were performed three times independently.

Microscope imaging

Saos-2 cells were cultured and exposed to the various concentrations of metal nanoparticles as stated above in 24-well plates; after the required exposure time cells were at first washed thoroughly three times in PBS. For the staining of the F-actin cytoskeleton and nuclei, cells were fixed with 3.7% (w/v) formaldehyde in PBS at room Temperature for 5 min and permeabilised with 0.1% Triton X-100 at room Temperature for 5 min. Then cells were stained with 50mg/L of tetramethyl rhodamine B isothiocyanate-conjugated phalloidin (Sigma-Aldrich, St. Louis, MO, USA) for 40 minutes at room temperature, followed by incubation with 5mg/L of trihydrochloride Hoechst 33342 (Thermo Fisher Scientific, Eugene, OR, USA) for 10 minutes in the dark. After washing with PBS, samples were mounted and examined using LSM 880 upright confocal laser scanning microscope with Airyscan (Zeiss, Oberkochen, Germany) for visualization of the staining with a 63X magnification objective. Processing of the obtained images was conducted using ZEN imaging software (Zeiss). λ_{ex} 540-545 nm and λ_{ex} 340 nm; λ_{em} 570-573 nm and λ_{em} 488 nm for tetramethyl rhodamine B isothiocyanate-conjugated phalloidin and Hoechst, respectively.

Flow-Cytometry

Apoptosis in Saos-2 cells after exposure to nanoparticles was determined using Annexin V-FITC Apoptosis Detection Kit (Sigma, UK) through flow-cytometry (BD FACSVerse™). Two fluorescent stains were used: Annexin V-FITC (Ex 480nm / Em 520 nm) and Propidium Iodide (Ex 520nm / Em 615nm).

Cells were prepared as previously described; after the chosen contact time with the nanoparticles cells were washed with PBS, trypsinised and resuspended in PBS. 1 ml

of this cells suspension was placed into Eppendorf and centrifuged at 4 °C, for 5 minutes at 1800 rpm (363 g). The supernatant was removed and the pellet of cells in re-suspended in 500 µl of annexin-binding buffer. After 30 min of incubation, 10 µl of annexin V–FITC and 5 µl of PI were added and the samples were incubated for another 30 min in the dark at room temperature prior to analysis.

Data collected were then analysed using FlowJo software (LLC, Data Analysis Software, Oregon, USA) to generate four quadrant plots.

Statistical analysis

Comparison of the effects of Cobalt and Titanium nanoparticles on the biophysical property of Saos-2 cells was performed using ANOVA test followed by Tukey's *post hoc* test of individual pair of data sets ($p < 0.05$). The Kruskal-Wallis test, followed by Dunn's test *post hoc* for the individual pairs of data sets, was used to compare the adhesive force measurements. All statistical analysis was performed using SPSS.

Acknowledgements

The authors would like to acknowledge Welsh Government (NRN156) and Arthritis Research UK (ARUK: 18461).

References

- [1] Saldaña L, Bensiamar F, Boré A, Vilaboa N. In search of representative models of human bone-forming cells for cytocompatibility studies. *Acta Biomaterialia*. 2011;7(12):4210-21.
- [2] Ahmad M, McCarthy M, Gronowicz G. An in vitro model for mineralization of human osteoblast-like cells on implant materials. *Biomaterials*. 1999;20(3):211-20.
- [3] Prokopovich P. Interactions between mammalian cells and nano- or micro-sized wear particles: Physico-chemical views against biological approaches. *Advances in Colloid and Interface Science* 2014;213:36-47
- [4] Xia Z, Ricciardi BF, Liu Z, von Ruhland C, Ward M, Lord A, Hughes L, Goldring SR, Purdue E, Murray D, Perino G. Nano-analyses of wear particles from metal-on-metal and non-metal-on-metal dual modular neck hip arthroplasty. *Nanomedicine* 2017;13(3):1205-1217
- [5] Buly RL, Huo MH, Salvati E, Brien W, Bansal M. Titanium wear debris in failed cemented total hip arthroplasty: An analysis of 71 cases. *The Journal of Arthroplasty*. 1992;7(3):315-23.
- [6] Schoon J, Geissler S, Traeger J, Luch A, Tentschert J, Perino G, Schulze F, Duda GN, Perka C, Rakow A. Multi-elemental nanoparticle exposure after tantalum component failure in hip arthroplasty: In-depth analysis of a single case. *Nanomedicine*. 2017;13(8):2415-2423
- [7] Margevicius KJ, Bauer TW, McMahon JT, Brown SA, Merritt K. Isolation and characterization of debris in membranes around total joint prostheses. *The Journal of bone and joint surgery American volume*. 1994;76(11):1664-75.

- [8] Saldaña L, Vilaboa N. Effects of micrometric Titanium particles on osteoblast attachment and cytoskeleton architecture. *Acta Biomaterialia*. 2010;6(4):1649-60.
- [9] Li C-y, Gao S-y, Terashita T, Shimokawa T, Kawahara H, Matsuda S, et al. In vitro assays for adhesion and migration of osteoblastic cells (Saos-2) on Titanium surfaces. *Cell Tissue Res*. 2006;324(3):369-75.
- [10] Dillon J, Waring-Green V, Taylor A, Wilson PM, Birch M, Gartland A, et al. Primary Human Osteoblast Cultures. In: Helfrich MH, Ralston SH, editors. *Bone Research Protocols. Methods in Molecular Biology*. 816: Humana Press; 2012. p. 3-18.
- [11] Brien WW, Salvati EA, Betts F, Bullough P, Wright T, Rimnac C, et al. Metal levels in cemented total hip arthroplasty. A comparison of well-fixed and loose implants. *Clinical orthopaedics and related research*. 1992(276):66-74.
- [12] Abu-Amer Y, Darwech I, Clohisy JC. Aseptic loosening of total joint replacements: mechanisms underlying osteolysis and potential therapies. *Arthritis Research & Therapy*. 2007;9(Suppl 1):S6-S.
- [13] Bahraminasab M, Sahari BB, Edwards KL, Farahmand F, Arumugam M, Hong TS. Aseptic loosening of femoral components – A review of current and future trends in materials used. *Materials & Design*. 2012;42(0):459-70.
- [14] Cadosch D, Chan E, Gautschi OP, Filgueira L. Metal is not inert: Role of metal ions released by biocorrosion in aseptic loosening—Current concepts. *Journal of Biomedical Materials Research Part A*. 2009;91A(4):1252-62.
- [15] Pioletti DP, Takei H, Kwon SY, Wood D, Sung KL. The cytotoxic effect of Titanium particles phagocytosed by osteoblasts. *J Biomed Mater Res*. 1999;46(3):399-407.

- [16] Rodan SB, Imai Y, Thiede MA, Wesolowski G, Thompson D, Bar-Shavit Z, et al. Characterization of Human Osteosarcoma Cell Line (Saos-2) with Osteoblastic Properties. *American Association for Cancer Research*. 1987;47:4961-6.
- [17] Pautke C, Schieker M, Tischer T, Kolk A, Neth P, Mutschler W, et al. Characterization of Osteosarcoma Cell Lines MG-63, Saos-2 and U-2 OS in Comparison to Human Osteoblasts. *Anticancer Research*. 2004;24:3743-8.
- [18] Ahmad M, Gawronski D, Blum J, Goldberg J, Gronowicz G. Differential response of human osteoblast-like cells to commercially pure (cp) Titanium grades 1 and 4. *Journal of Biomedical Materials Research*. 1999;46(1):121-31.
- [19] Degasne I, Basle MF, Demais V, Hure G, Lesourd M, Grolleau B, et al. Effects of roughness, fibronectin and vitronectin on attachment, spreading, and proliferation of human osteoblast-like cells (Saos-2) on Titanium surfaces. *Calcif Tissue Int*. 1999;64(6):499-507.
- [20] Harmand MF. In vitro study of biodegradation of a Co-Cr alloy using a human cell culture model. *J Biomater Sci Polym Ed*. 1995;6(9):809-14.
- [21] Lohmann CH, Schwartz Z, Köster G, Jahn U, Buchhorn GH, MacDougall MJ, et al. Phagocytosis of wear debris by osteoblasts affects differentiation and local factor production in a manner dependent on particle composition. *Biomaterials*. 2000;21(6):551-61.
- [22] Allen MJ, Myer BJ, Millet PJ, Rushton N. The Effects of Particulate Cobalt, Chromium and Cobalt-Chromium Alloy on Human Osteoblast-like cells in vitro. *British Editorial Society of Bone and Joint Surgery*. 1997;79-B(3):475-82.
- [23] Zijlstra WP, Bulstra SK, van Raay JJ, van Leeuwen BM, Kuijjer R. Cobalt and chromium ions reduce human osteoblast-like cell activity in vitro, reduce the OPG to RANKL ratio, and induce oxidative stress. *J Orthop Res*. 2012;30(5):740-7.

- [24] Gregory CA, Grady Gunn W, Peister A, Prockop DJ. An Alizarin red-based assay of mineralization by adherent cells in culture: comparison with cetylpyridinium chloride extraction. *Analytical Biochemistry*. 2004;329(1):77-84.
- [25] Preedy EC, Brousseau E, Evans SL, Perni S, Prokopovich P. Adhesive forces and surface properties of cold gas plasma treated UHMWPE. *Colloids Surf A Physicochem Eng Asp*. 2014;460:83-9.
- [26] Sader JE, Larson I, Mulvaney P, White LR. Method for the calibration of atomic force microscope cantilevers. *Review of Scientific Instruments*. 1995;66(7):3789-98.
- [27] Sader JE, Sanelli JA, Adamson BD, Monty JP, Wei X, Crawford SA, et al. Spring constant calibration of atomic force microscope cantilevers of arbitrary shape. *Review of Scientific Instruments*. 2012;83(10):103705--16.
- [28] Sneddon IN. The relation between load and penetration in the axisymmetric boussinesq problem for a punch of arbitrary profile. *International Journal of Engineering Science*. 1965;3(1):47-57.
- [29] Nine M, Choudhury D, Hee A, Mootanah R, Osman N. Wear Debris Characterization and Corresponding Biological Response: Artificial Hip and Knee Joints. *Materials*. 2014;7(2):980-1016.
- [30] Prokopovich P. Interactions between mammalian cells and nano- or micro-sized wear particles: Physico-chemical views against biological approaches. *Advances in Colloid and Interface Science*. 2014;213(0):36-47.
- [31] Howling GI, Sakoda H, Antonarulrajah A, Marrs H, Stewart TD, Appleyard S, et al. Biological Response to Wear Debris Generated in Carbon Based Composites as Potential Bearing Surfaces for Artificial Hip Joints. *Biomed Mater Res Part B: Appl Biomater*. 2003;67(B):758-64.

- [32]da Rosa ELS. Kinetic effects of TiO₂ fine particles and nanoparticles aggregates on the nanomechanical properties of human neutrophils assessed by force spectroscopy. *BMC Biophysics*. 2013;6:11-.
- [33]Ingham E, Fisher J. The role of macrophages in osteolysis of total joint replacement. *Biomaterials*. 2005;26(11):1271-86.
- [34]Callaghan JJ, O'rourke MR, Saleh KJ. Why knees fail: Lessons learned. *Journal of Arthroplasty*. 2004;19:31-4.
- [35]Papageorgiou I, Yin Z, Ladon D, Baird D, Lewis AC, Sood A, et al. Genotoxic effects of particles of surgical Cobalt chrome alloy on human cells of different age in vitro. *Mutation Research/Fundamental and Molecular Mechanisms of Mutagenesis*. 2007;619(1–2):45-58.
- [36]E. Callard Preedy, S. Perni, P. Prokopovich "Cobalt and Titanium Nanoparticles Influence on Mesenchymal Stem Cell Interfacial Properties" *Coll. Surfaces B* 2017;157:146-156
- [37]E. Callard Preedy, S. Perni, P. Prokopovich "Cobalt, Titanium and PMMA Bone Cement Debris Influence on Mouse Osteoblasts Cell Elasticity, Spring constant and Calcium Production Activity" *RSC Advances* 2015;5:83885-83898
- [38]Rakow A, Schoon J, Dienelt A, John T, Textor M, Duda G, Perka C, Schulze F, Ode A. Influence of particulate and dissociated metal-on-metal hip endoprosthesis wear on mesenchymal stromal cells in vivo and in vitro. *Biomaterials*. 2016;98:31-40
- [39]Pioletti DP, Leoni L, Genini D, Takei H, Du P, Corbeil J. Gene expression analysis of osteoblastic cells contacted by orthopedic implant particles. *J Biomed Mater Res*. 2002 Sep 5;61(3):408-420.

- [40] Vandrovcova M, Jirka I, Novotna K, Lisa V, Frank O, Kolska Z, et al. Interaction of human osteoblast-like Saos-2 and MG-63 cells with thermally oxidized surfaces of a Titanium-niobium alloy. *PLoS One*. 2014;9(6):e100475.
- [41] Perni S., Callard Preedy E., Prokopovich P. Success and Failure of Colloidal Approached in Bacterial Adhesion. *Adv. Coll. Interface Sci*. 2014;206:265-274
- [42] Baxter LC, Frauchiger V, Textor M, ap Gwynn I, Richards RG. Fibroblast and osteoblast adhesion and morphology on calcium phosphate surfaces. *European cells & materials*. 2002;4:1-17.
- [43] Yim EKF, Darling EM, Kulangara K, Guilak F, Leong KW. Nanotopography-induced changes in focal adhesions, cytoskeletal organization, and mechanical properties of human mesenchymal stem cells. *Biomaterials*. 2010;31(6):1299-306.
- [44] Callard Preedy E., Perni S., Prokopovich P. Nanomechanical and Surface Properties of rMSCs post Exposure to CAP Treated UHMWPE Wear Particles. *Nanomed.: Nanotech. Biol. Med*. 2016;12:723-734
- [45] Darling EM, Topel M, Zauscher S, Vail TP, Guilak F. Viscoelastic properties of human mesenchymally-derived stem cells and primary osteoblasts, chondrocytes, and adipocytes. *Journal of Biomechanics*. 2008;41(2):454-64.
- [46] Thoumine O, Cardoso O, Meister JJ. Changes in the mechanical properties of fibroblasts during spreading: a micromanipulation study. *European biophysics journal* 1999;28(3):222-34
- [47] Domke J, Dannöhl S, Parak WJ, Müller O, Aicher WK, Radmacher M. Substrate dependent differences in morphology and elasticity of living osteoblasts

- investigated by atomic force microscopy. *Colloids and Surfaces B: Biointerfaces*. 2000;19(4):367-79.
- [48] Docheva D, Padula D, Popov C, Mutschler W, Clausen-Schaumann H, Schieker M. Researching into the cellular shape, volume and elasticity of mesenchymal stem cells, osteoblasts and osteosarcoma cells by atomic force microscopy. *Journal of Cellular and Molecular Medicine*. 2008;12(2):537-52.
- [49] Discher DE, Janmey P, Wang YL. Tissue cells feel and respond to the stiffness of their substrate. *Science*. 2005;310(5751):1139-43.
- [50] Engler A, Sen S, Sweeney H, Discher D. Matrix elasticity directs stem cell lineage specification. *Cell*. 2006;126(4):677 - 89.
- [51] Wells RG. The role of matrix stiffness in regulating cell behavior. *Hepatology*. 2008;47(4):1394-400.
- [52] Tee S-Y, Fu J, Chen Christopher S, Janmey Paul A. Cell Shape and Substrate Rigidity Both Regulate Cell Stiffness. *Biophysical Journal*. 2011;100(5):L25-L7.
- [53] Kasza KE, Nakamura F, Hu S, Kollmannsberger P, Bonakdar N, Fabry B, et al. Filamin A is essential for active cell stiffening but not passive stiffening under external force. *Biophys J*. 2009;96(10):4326-35.
- [54] Bhadriraju K, Hansen LK. Extracellular Matrix- and Cytoskeleton-Dependent Changes in Cell Shape and Stiffness. *Experimental Cell Research*. 2002;278(1):92-100.
- [55] Bacabac RG, Mizuno D, Schmidt CF, MacKintosh FC, Van Loon JJWA, Klein-Nulend J, et al. Round versus flat: Bone cell morphology, elasticity, and mechanosensing. *Journal of Biomechanics*. 2008;41(7):1590-8.
- [56] Assoian RK, Klein EA. Growth control by intracellular tension and extracellular stiffness. *Trends in Cell Biology*. 2008;18(7):347-52.

Table 1. Zeta potential and size of nanoparticles and zeta potential of Saos-2 cells measured in media solution along with their pH values.

Nanoparticles	pH	Zeta Potential (mV)
Co 30nm	8.33	-19.4±1.0
Ti 30nm	7.07	-44.7±1.9
Saos-2 cells		-7.70±0.6

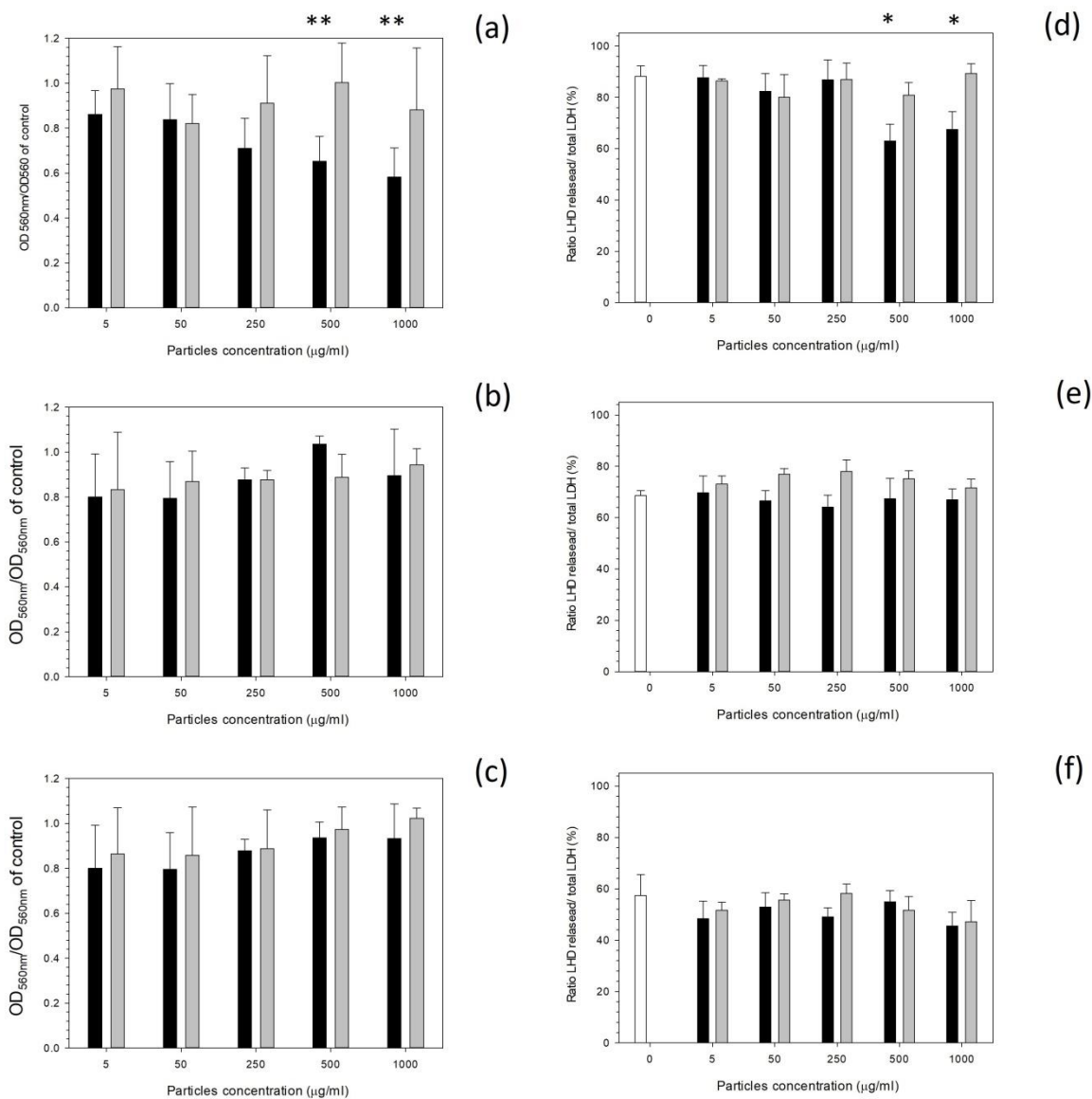


Figure 1. Cell Viability results (MTT assay on left side and LHD on right side) of Saos-2 cells (n =6) exposed to Cobalt (black columns) and Titanium (grey columns) elemental nanoparticles at (a, d) 24h, (b, e) 48h, and (c, f) 72h. * p<0.05 and ** p<0.01

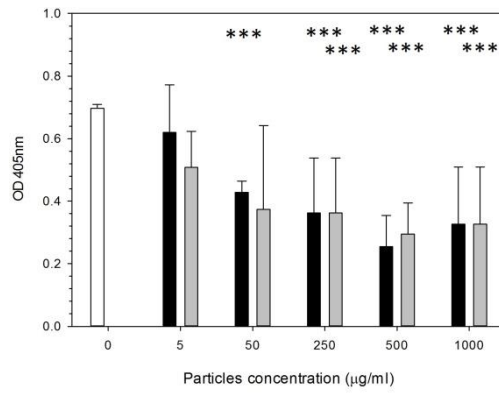


Figure 2. Saos-2 cells (n = 6) osteoblast mineralisation ability post exposure to Cobalt (black columns) and Titanium (grey columns) nanoparticles. ***p<0.005.

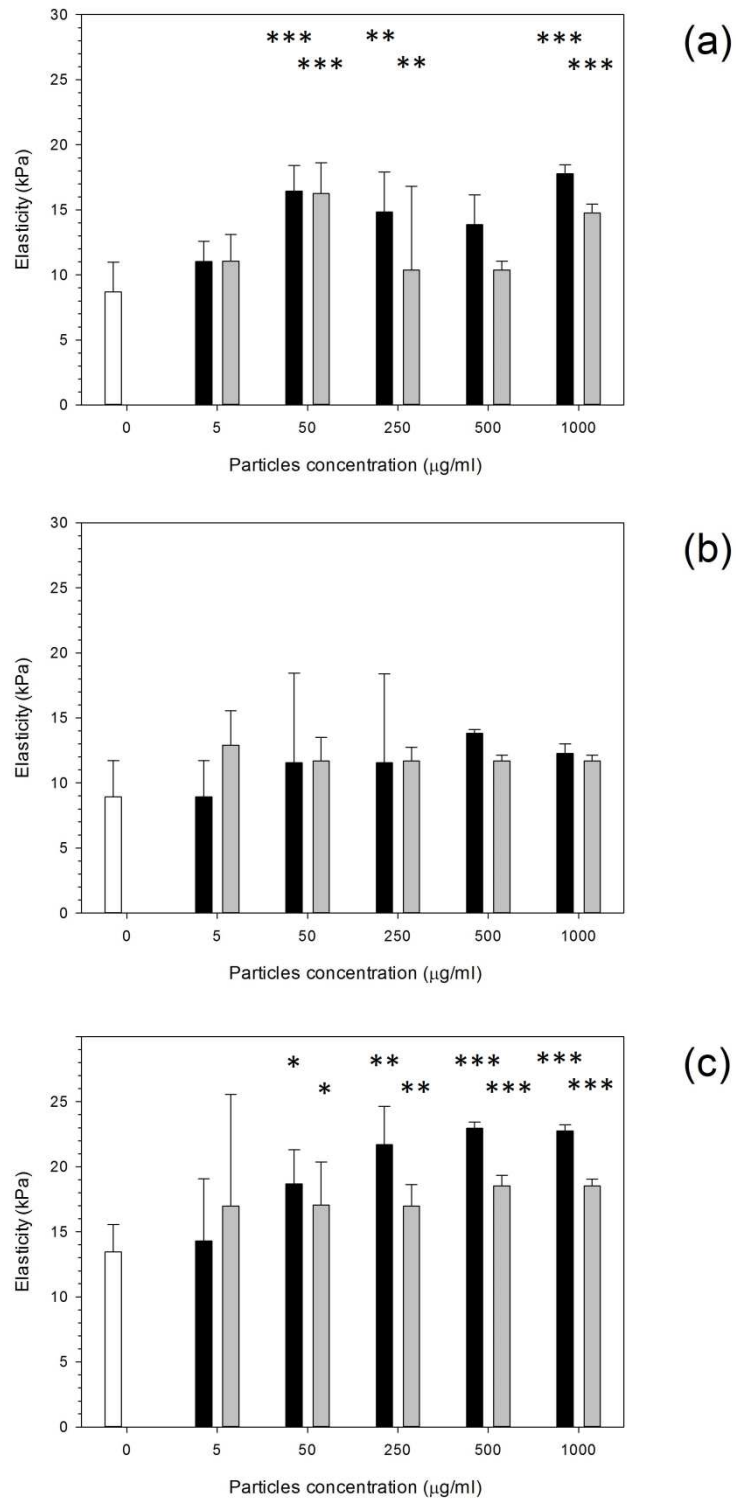


Figure 3. Mean cell elasticity of Saos-2 cells (n = 30) exposed to Cobalt (black columns) and Titanium (grey columns) nanoparticles at three time points: (a) 24h, (b) 48h, and (c) 72h. *p<0.05, ** p<0.01 and ***p<0.005.

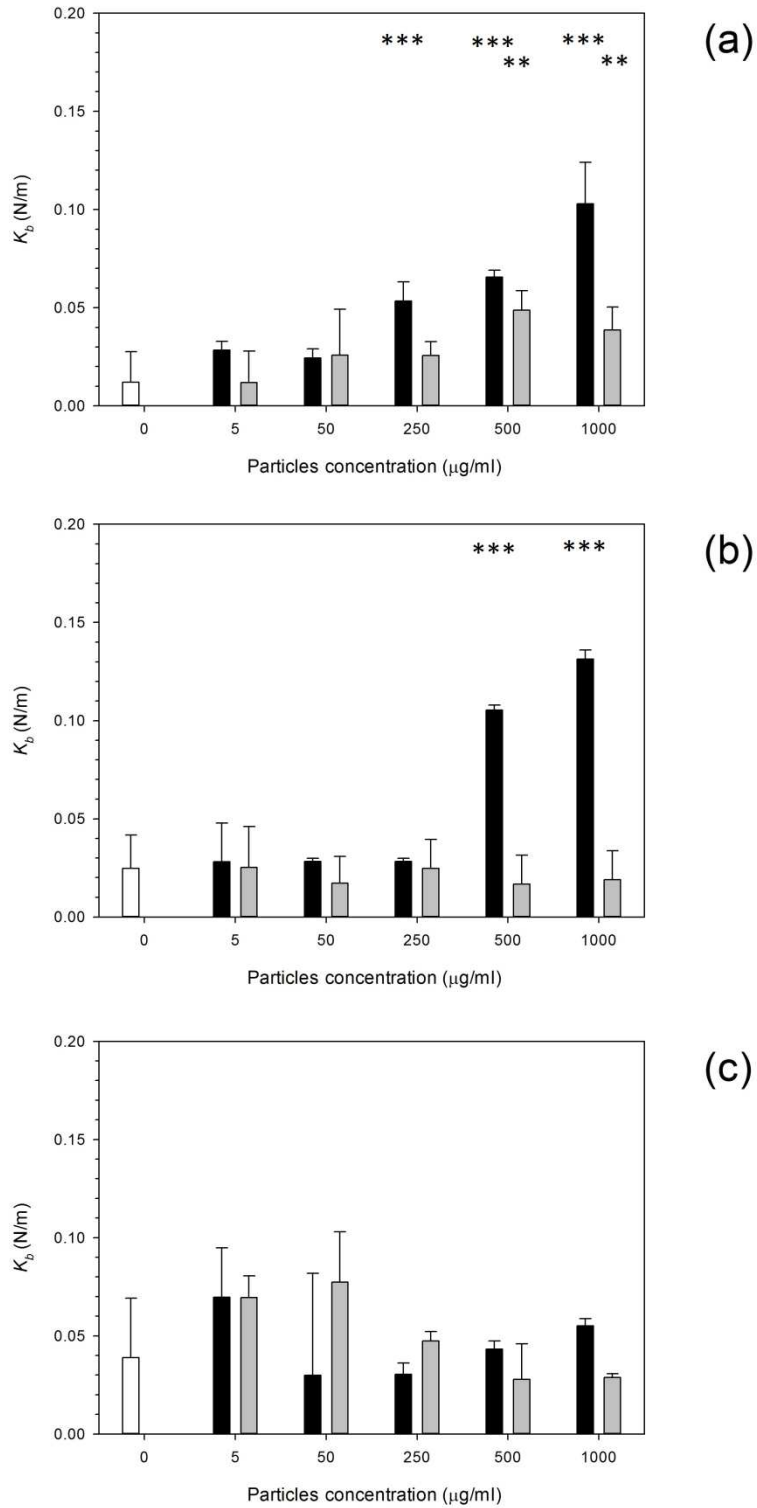


Figure 4. Median spring constant of Saos-2 cells (n = 30) exposed Cobalt (black columns) and Titanium (grey columns) nanoparticles at each time point: (a) 24h, (b) 48h, and (c) 72h. * $p < 0.05$, ** $p < 0.01$ and *** $p < 0.005$.

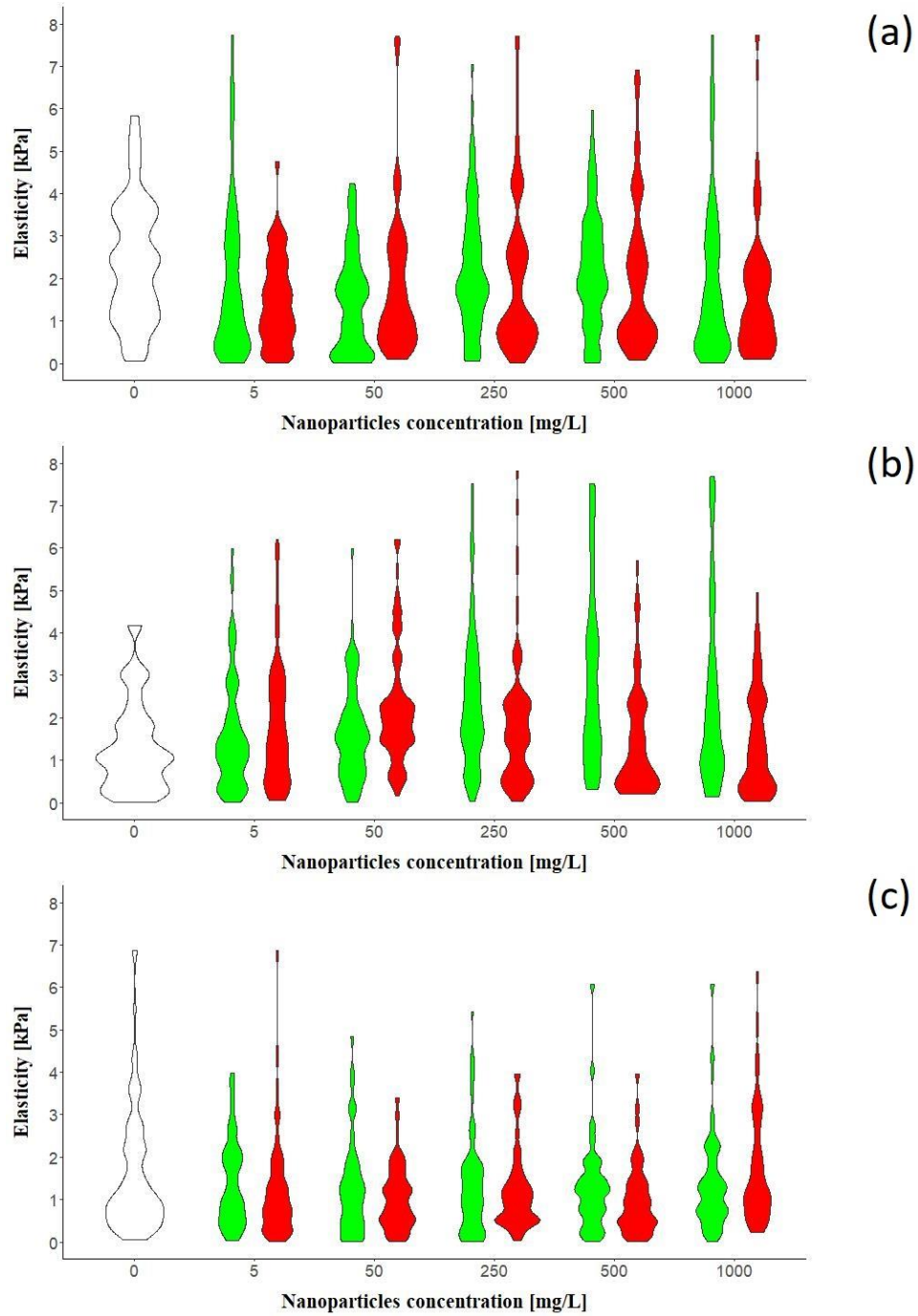


Figure 5. Violin plots of adhesion force distribution of Saos-2 cells ($n = 30$) exposed to Cobalt (green) and Titanium (red) nanoparticles for all time points (controls in white columns): (a) 24h, (b) 48h, and (c) 72h.

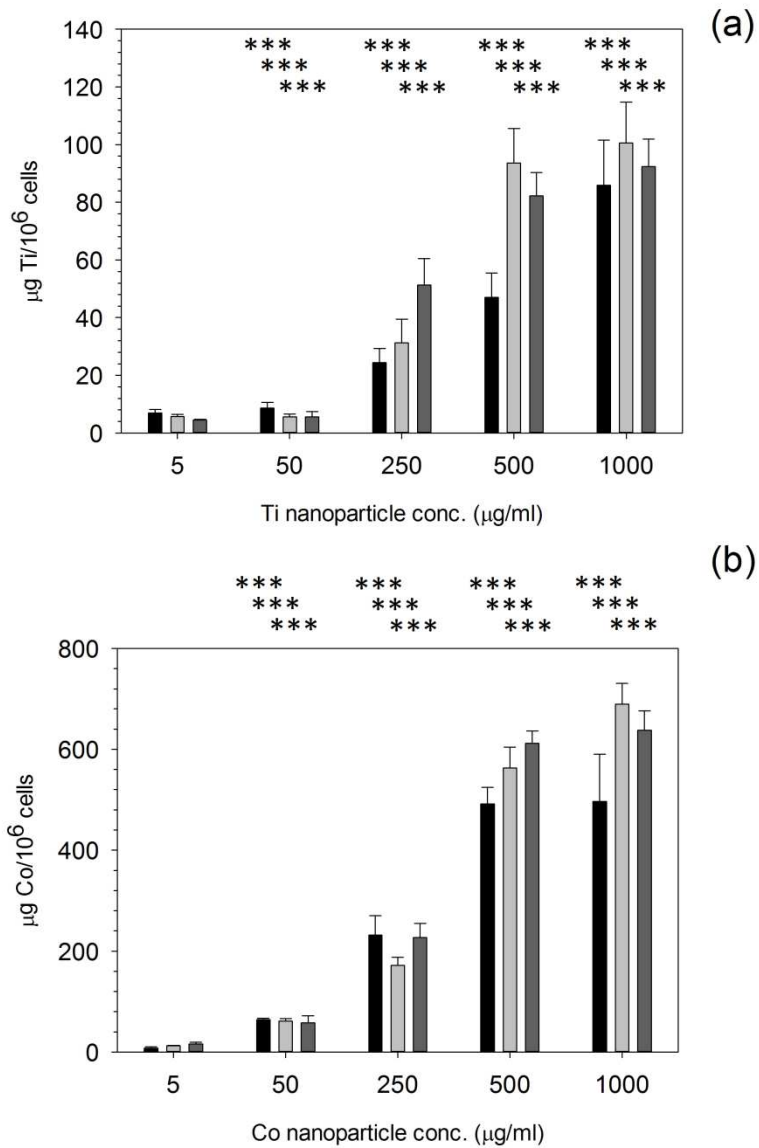


Figure 6. Saos-2 cells (n = 6) uptake of Titanium (a) and Cobalt (b) ions from corresponding nanoparticles after exposure from 24 h (■), 48 h (▒) and 72 h (▓) at various nanoparticles concentrations. * p<0.05, ** p<0.01 and ***p<0.005.

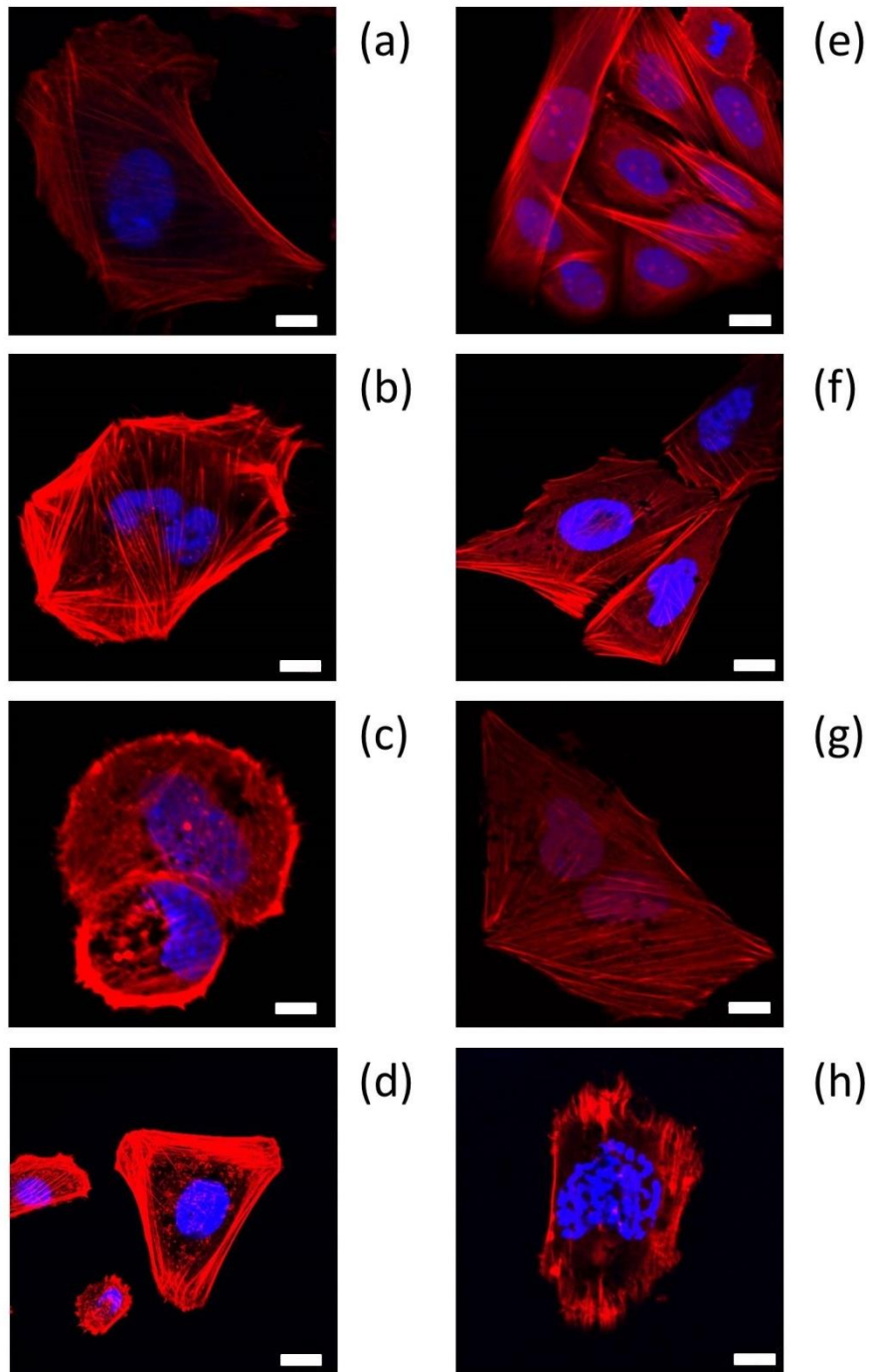


Figure 7. Microscope images of Saos-2 cells stained with phalloidin (actin) in red and DAPI in blue exposed to Co nanoparticles. Left side images correspond to 1 day and right side images correspond to 3 days exposure. (a) and (e) control samples (0 mg/ml), (b) and (f) 50 $\mu\text{g/ml}$, (c) and (g) 500 $\mu\text{g/ml}$, (d) and (h) 1000 $\mu\text{g/ml}$. bar represent 10 μm .

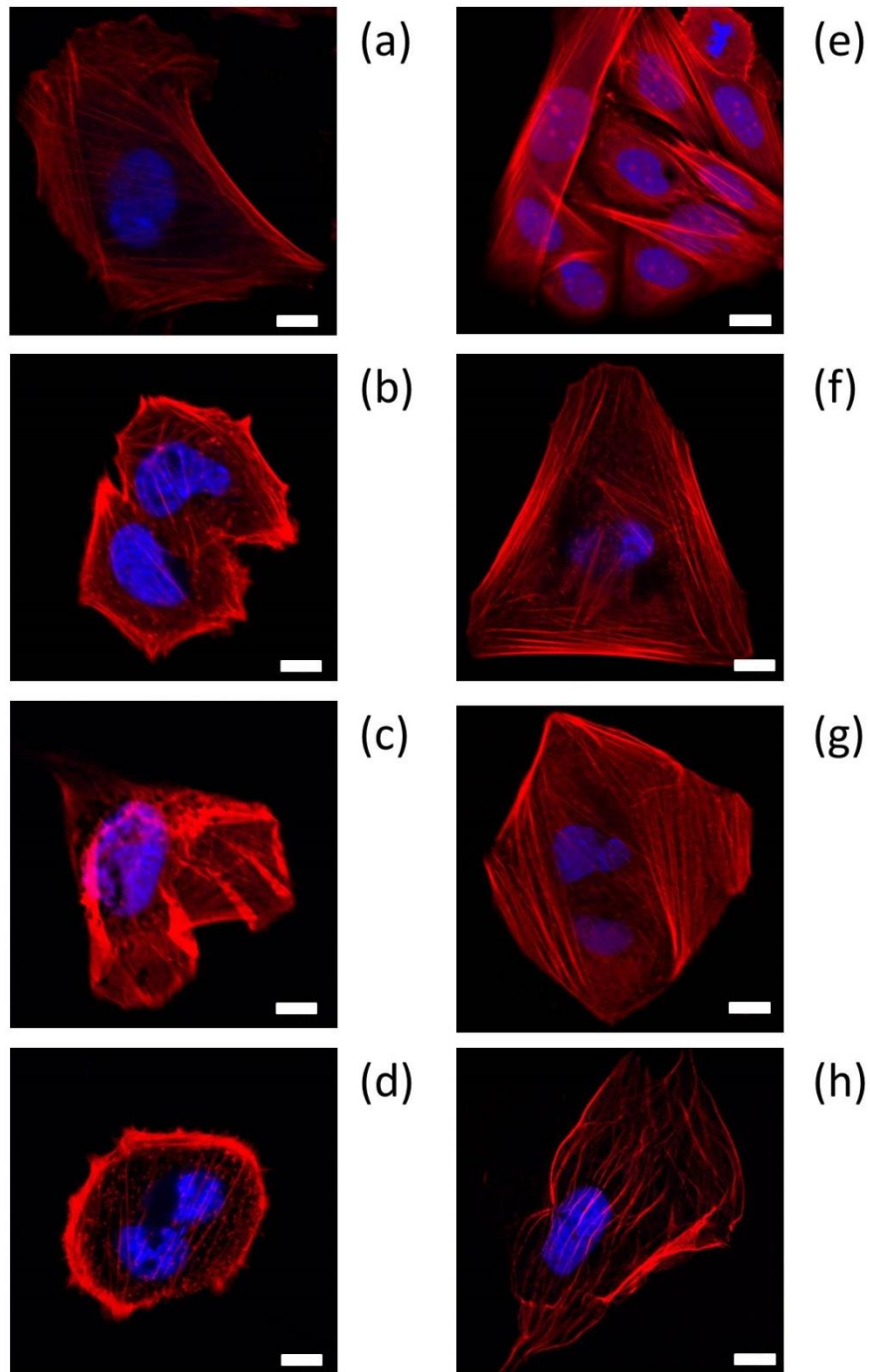


Figure 8. Microscope images of Saos-2 cells stained with phalloidin (actin) in red and DAPI in blue exposed to Ti nanoparticles. Left side images correspond to 1 day and right side images correspond to 3 days exposure. (a) and (e) control samples (0 mg/ml), (b) and (f) 50 $\mu\text{g/ml}$, (c) and (g) 500 $\mu\text{g/ml}$, (d) and (h) 1000 $\mu\text{g/ml}$. bar represent 10 μm .

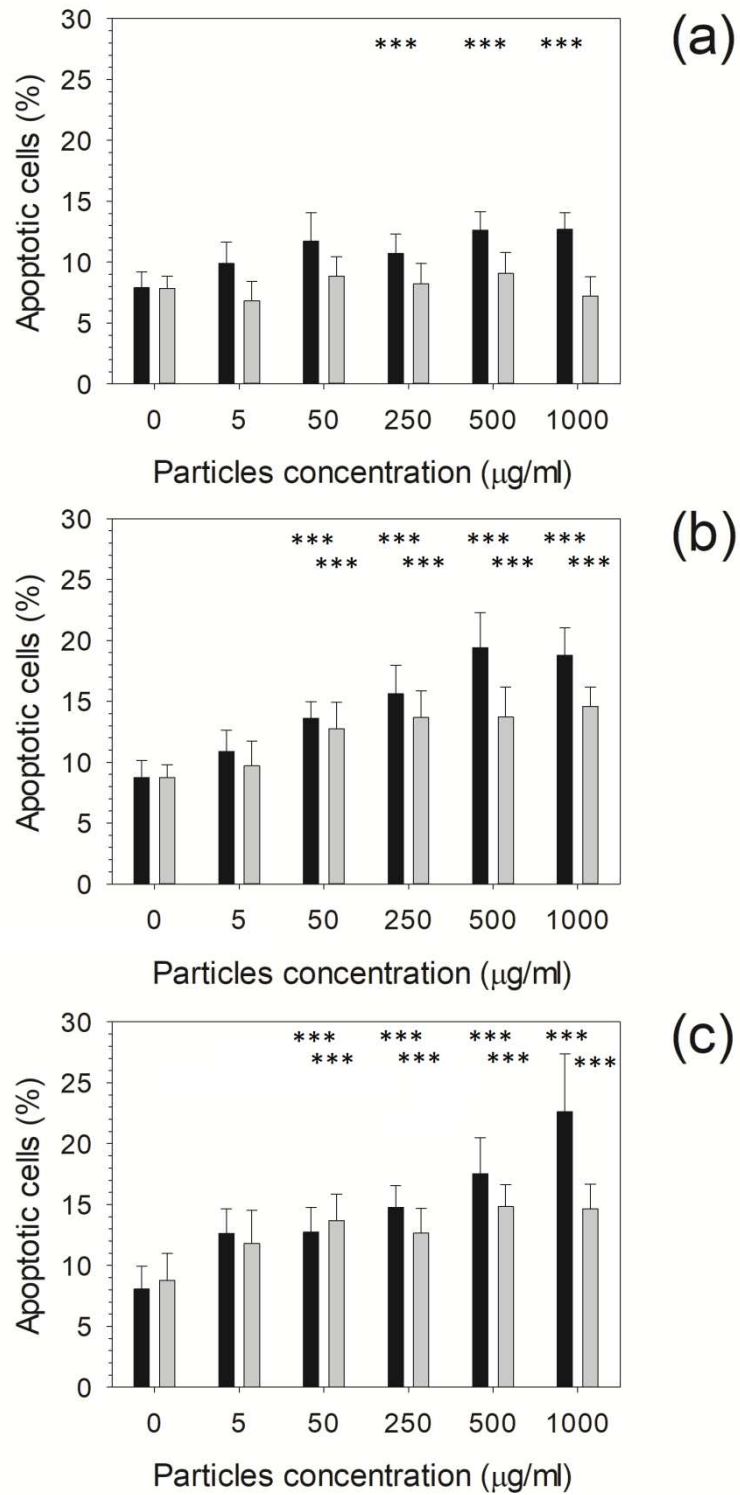


Figure 9. Percentage of apoptotic Saos-2 cells (n = 6) after exposure to Cobalt (black column) and Titanium (grey column) elemental nanoparticles for (a) 24h, (b) 48h, and (c) 72 h.